Theoretical approach to magnetic force microscopy

A. Wadas* and P. Grütter
Institut für Physik, Klingelbergstrasse 82, 4056 Basel, Switzerland
(Received 13 October 1988)

This paper presents an analytical approach to magnetic force microscopy (MFM). Some features of a realistic magnetic tip, modeled by a truncated pyramid, have been studied theoretically. By use of analytical formulas to describe the magnetic field above a sample with periodic domains and perpendicular anisotropy, tip-sample interaction has been calculated as a function of tip geometry and tip-sample distance. Lateral resolution and sensitivity are related to the geometrical parameters that describe the shape of the tip, which leads to the surprising result that it is not the tip with the smallest tip radius that gives rise to the highest lateral resolution in MFM. Depending on the tip volume, the force sensitivity can vary by more than a factor of 3. The lateral resolution is shown to decrease, as expected, with increasing tip-sample separation. The theoretical results presented here are of relevance for the interpretation and comparison of experimental results. For a tip of given geometry and magnetization, the results of this paper allow the determination of the expected lateral resolution and sensitivity as a function of tip-sample separation.

I. INTRODUCTION

Atomic force microscopy (AFM) (Ref. 1) has been applied to magnetic samples for the first time by Martin *et al.*[2] and Saenz *et al.*[3] The sensor in magnetic force microscopy (MFM) consists of a sharp magnetic tip mounted on a cantilever. Forces acting on the tip cause a deflection of the cantilever which can be measured by electron tunneling[1,3] or by interferometry.[2,4] The measured interaction forces depend on the magnetic structure of the sample and the physical properties, such as magnetization and geometry, of the tip. Up to now, some effort has been made to study experimentally the stray fields from a magnetic recording head,[2] an isolated domain wall,[3] or whole domains.[4–7] Theoretically, MFM has been investigated by a number of previous authors for various magnetizations of tip and sample.[3,8–13] Recently, samples which are interesting as novel recording media with perpendicular anisotropy have been investigated in MFM experiments.[4,7,14] For such cases the magnetic contrast has been calculated earlier.[10,11]

The aim of this paper is to continue previous work, calculating the magnetic contrast of samples with perpendicular anisotropy in MFM experiments as a function of tip geometry and tip-sample separation, and to present a completely analytical approach. The paper is organized as follows: First, an expression is given for the magnetic field above the sample. Then the force acting on a tip modeled by a truncated pyramid is derived. We then simulate the effect of geometrical tip parameters on the lateral resolution and the force sensitivity. Finally, the lateral resolution as a function of tip-sample distance with optimized geometrical tip parameters is presented.

II. RESULTS AND DISCUSSION

In MFM the magnetic tip is scanned over the surface of a sample and interacts with the magnetic field produced by the sample. The energy of such an interaction is described by

$$E = -\int_{\text{tip}}\int\int \mathbf{H}(\mathbf{r})\mathbf{M}\,dV\ , \tag{1}$$

where $\mathbf{M}$ is the tip magnetization and $\mathbf{H}(\mathbf{r})$ is the magnetic field above a sample. A uniformly magnetized tip is assumed. In the experiment, the magnetic tip has one degree of freedom which we define as the z axis. The force acting on the tip in the direction of the z axis is related to the interaction energy

$$F_z = -\frac{\partial E}{\partial z}\ . \tag{2}$$

The magnetic field used in formula (1) is created by the magnetization distribution in the sample. Let us assume that our sample is a thin film with the thickness a and infinite dimensions in all other directions. Figure 1 shows such a sample with the chosen coordinate system. We assume that there is a stripe domain structure with anisotropy perpendicular to the sample surface. Domains have the same width and a periodicity D. The magnetic field H outside such a sample was presented earlier,[10,11]

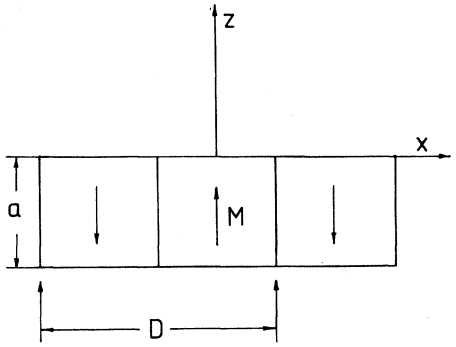

FIG. 1. Domain structure with the coordinate system.

$$\begin{bmatrix} H_x \\ H_y \\ H_z \end{bmatrix} = 8M_s \sum_{n=0}^{\infty} \frac{(-1)^n}{(2n+1)} \left[1-\exp\left[-(2n+1)\frac{2\pi a}{D}\right]\right] \exp\left[-(2n+1)\frac{2\pi z}{D}\right] \begin{bmatrix} \sin\left[(2n+1)\frac{2\pi x}{D}\right] \\ 0 \\ \cos\left[(2n+1)\frac{2\pi x}{D}\right] \end{bmatrix}, \tag{3}$$

where M_s is the magnetization of the sample.

Using this formula in further calculations, we neglect disturbances in the field caused by the presence of a tip and any changes inside the tip caused by the sample. In previous papers the tip had the shape of a cylinder terminated by a hemisphere.[10,11] Now we assume that it has the shape of a truncated pyramid. Figure 2 sketches this case. Such a shape is more similar to the real shape of the electrochemically etched tips used in MFM. Electrochemically etched tips are known to be described very well by a hyperboloid defined by the apex radius of curvature and the half angle of the shank.[15] A truncated pyramid is a good approximation of a hyperboloid and mathematically much more convenient. We use Eqs. (1), (2), and (3) to calculate the force acting on a tip. Noting the invariance of the stray field against y translations, we obtain the formula describing the force,

$$F(x,z)=2(\tan\alpha)\int_0^L dz'(z'+b)\int_{-(z'+b)\tan\alpha}^{(z'+b)\tan\alpha} dx' \left[M_x\frac{\partial}{\partial z}H_x(x+x',z+z')+M_z\frac{\partial}{\partial z}H_z(x+x',z+z')\right], \tag{4}$$

where M_x and M_z are the magnetization components of the tip. L, b, and α are defined in Fig. 2. Substituting H from formula (3), we can calculate the second integral,

$$F(x,z)=\sum_{n=0}^{\infty} S(M_s,M_x,M_z,a,D,\alpha)\int_0^L dz'(z'+b)\exp\left[-\frac{2\pi}{D}(2n+1)z'\right]\sin\left[\frac{2\pi}{D}(2n+1)(z'+b)\tan\alpha\right], \tag{5}$$

where

$$S(M_s,M_x,M_z,a,D,\alpha)=-32M_s(\tan\alpha)\frac{(-1)^n}{(2n+1)}\left[1-\exp\left[-(2n+1)\frac{2\pi a}{D}\right]\right]\exp\left[-(2n+1)\frac{2\pi z}{D}\right]$$
$$\times\left[M_z\cos\left[(2n+1)\frac{2\pi x}{D}\right]+M_x\sin\left[(2n+1)\frac{2\pi x}{D}\right]\right].$$

The last integral can be solved analytically,[16]

$$F(x,z)=\sum_{n=0}^{\infty} S(M_s,M_x,M_z,a,D,\alpha)\left[b\frac{\exp(pz')}{(p^2+r^2)}[p\sin(k)-r\cos(k)]\right.$$
$$+z'\frac{\exp(pz')}{(p^2+r^2)}[p\sin(k)-r\cos(k)]$$
$$\left.-\frac{\exp(pz')}{(p^2+r^2)^2}[(p^2-r^2)\sin(k)-2pr\cos(k)]\right]\Bigg|_0^L \tag{6}$$

with

$$p=-(2\pi/D)(2n+1),$$

$$r=(2\pi/D)(2n+1)\tan\alpha,$$

and

$$k=2\pi/D(2n+1)(z'+b)\tan\alpha.$$

We thus have reached our goal of deriving an analytical equation describing the magnetic forces acting on a tip. The sample is described by the magnetization M_s, the thickness a, and the domain structure period D, while the tip is characterized by its magnetization components M_x, M_z, the length L, the angle α, and the base length $2R_g$ (Fig. 2). Formula (6) is exact for the case of a magnetic stripe domain structure. Figure 3 presents data for

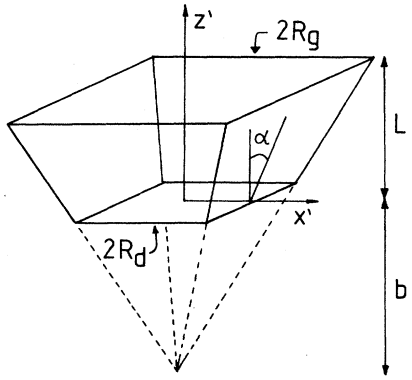

FIG. 2. Pyramidal tip model used for the calculations in the new coordinate system. L is the length of the tip.

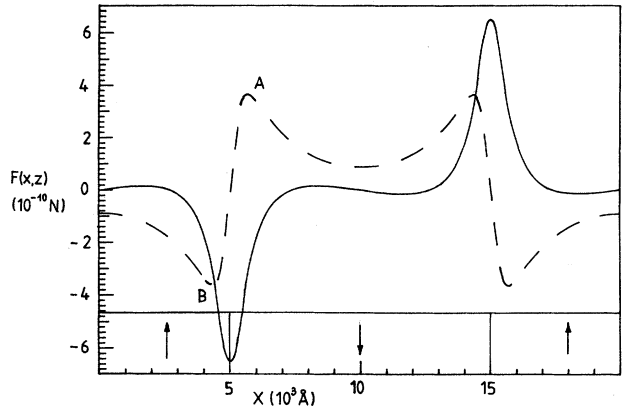

FIG. 3. Magnetic images for two cases: (dashed line) tip magnetization is directed perpendicularly to the sample surface (z axis); (solid line) tip magnetization is parallel to the sample surface (x axis). Height of scanning $z = 200$ Å.

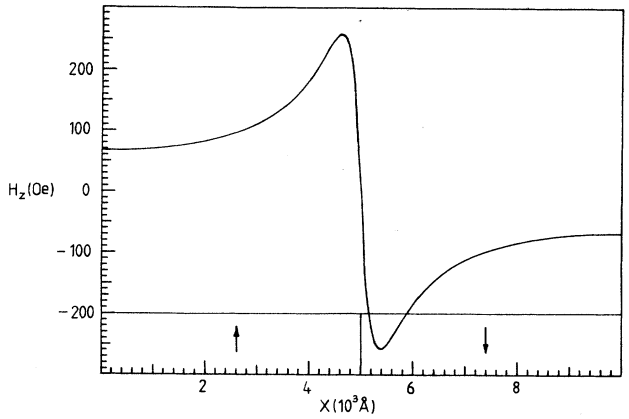

FIG. 4. Magnetic field H_z above the sample at $z = 200$ Å.

two cases, when the tip magnetization is along the x axis (solid line) and along the z axis (dashed line). We used the following numerical values: For $M_s = 109$ ergs/(G s cm^3)TbFe, $M_t = 1714$ ergs/(G s cm^3) for iron tip, $D = 20000$ Å, $a = 500$ Å, $L = 3000$ Å, $R_g = 900$ Å, $R_d = 400$ Å, and $z = 200$ Å. For a cylindrical-tip model the quantitative features of the force trace changes by less than 10% if the length L is changed from 3000 to 10^6 Å. In the first case (tip magnetization parallel to the sample surface), we note the asymmetry of the image which reflects the asymmetry of the configuration. The same contrast has recently been obtained experimentally by Rugar *et al.*[7] on Tb-Fe-Co alloy with a domain pattern comparable to Fig. 1. Unfortunately they only published qualitative data, so a more detailed, quantitative comparison with our theory is not possible.

Let us now focus our attention on the case when the tip magnetization is perpendicular to the sample surface. This case is represented by the dashed line in Fig. 3. Here, the symmetry of the tip-sample configuration is reflected in the obtained image. To understand this image, we plotted the field H_z above the sample at a distance $z = 200$ Å in Fig. 4. Qualitatively, this field can be described as follows. We can imagine two thin films magnetized perpendicular to the surface and opposite to each other, separated by a large distance between their edges. If this distance is decreased, the superposition of the stray fields of the two films will lead to the peak-peak structure observed in Fig. 4. The peak-peak distance is shortest if the film separation is zero, replicating our sample domain structure. We point out that the peak structures marked A and B in Fig. 3 are a reflection of the infinitely narrow domain wall. Therefore, the lateral separation between the peak A and the valley B (peak-valley separation AB) is a good measure of the lateral resolution. We expect that the contrast between peaks A and B will not be as pronounced above real domain walls of finite width. We define the peak-valley amplitude of the signal as the sensitivity over a domain wall. The sensitivity, thus defined, is directly related to the experimentally observable force contrast.

Generally, an infinitely small tip would lead to the highest lateral resolution. MFM tips are usually electrochemically etched from thin wires or foils. This determines the base length R_g. The length L can be controlled easily by bending the wire or foil. It is rather difficult, but not impossible, to control the length R_d precisely. Let us fix the length $L = 3000$ Å.

We can now ask what should the shape of the tip be in order to get the smallest peak-valley separation AB (i.e., the highest lateral resolution). To answer this question we fix the base length $R_g = 2100$ Å and the tip-sample separation $z = 1000$ Å. If the dimension R_d of the truncated pyramid is changed, this simultaneously will vary the angle α. We then calculate the peak-valley separation AB and the sensitivity values as a function of α. The results are shown in Fig. 5. The tip with the smallest tip length R_d is marked by an asterisk. It is surprising that the highest resolution is not obtained with a tip with zero tip length R_d. We define the angle related to the minimum peak-valley separation AB as the critical angle α_c. We can understand this phenomenon as follows: The final resolution is due to three different contributions to the force arising from the magnetic charges on the top (side length R_g), the base (with side length R_d), and the sides of the truncated pyramid. Keeping R_g and L constant and varying the angle α from the largest value to zero decreases the slope of the sides and thus improves the resolution. Simultaneously, the base length R_d increases from zero to R_g; this decreases resolution. For large angles α the improvement of resolution due to the effect from the sides of the pyramid dominates. For smaller angles α the increasing of R_d dominates and worsens the resolution. At the critical angle α_c both effects are balanced. The effect arising from the area defined by R_g is constant as L is constant.

Sensitivity decreases the smaller the length R_d is. This is clear as the whole volume of the tip also decreases. We point out the large sensitivity range from 1 to nearly 3.5×10^{-9} N.

Looking at Fig. 5 we can understand why it is so

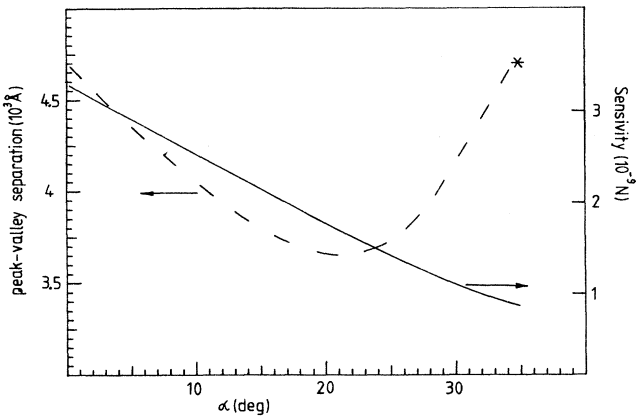

FIG. 5. Dependence of peak-valley separation AB and sensitivity vs angle α obtained with the tip described by $R_g = 2100$ Å, $L = 3000$ Å, and $z = 1000$ Å.

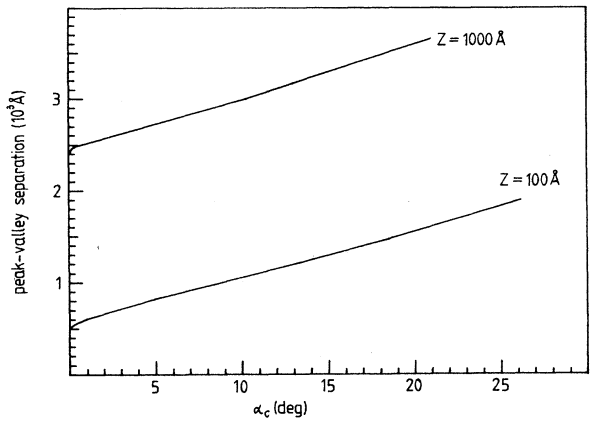

FIG. 7. Relation between critical angle α_c and peak-valley separation AB at two z levels.

difficult to compare the experimental results of different authors. For the same ratio R_g/L, resolution and sensitivity strongly depend on the angle α. The angle α of the tips has to be very well controlled in order to achieve quantitative reproducibility of results measured by different tips.

We expect that tips at a fixed z level with different R_g/L values have different critical angles. This is confirmed by calculations. Figure 6 shows the dependence of critical angle α_c versus the ratio R_g/L for fixed L and two different z levels of the tip. It is interesting that this dependence is nearly linear with the same slope independent of z. We find a similar functional dependence when we plot the peak-valley separation AB versus critical angle. Nearly linear curves with the same slope at two different z levels have been obtained (Fig. 7). We see from both Figs. 6 and 7 that the critical angle is a very important feature describing the tip. For a given tip with a given R_g/L value the critical angle α_c can be determined from Fig. 6. This then allows the determination of the maximum resolution at a certain distance z (Fig. 7). In the experiment, it is very important how the resolution changes with the z level.

Let us consider the case with fixed length $L = 3000$ Å and $R_g = 900$ Å. At each z level we calculate the critical angle and the minimal peak-valley separation AB. These data are plotted in Fig. 8. The resolution strongly depends on the scan height z. When scanning closer to the surface a sharper tip is necessary to obtain the highest resolution while at distances of more than 1000 Å the tip should be more parallelepiped than pyramidal. It seems theoretically possible to obtain a peak-valley separation of better than 500 Å with uniformly magnetized tips operated close to the sample (Fig. 7). However, as has been pointed out,[10,13,17] it is not possible to scan the sample very close to the surface because of the influence of the tip on the sample. The magnetic stray field produced by the tip is large at such a small distance and it can destroy the magnetic structure of the sample. If the coercivity and magnetization of the sample are known, we can estimate the tip-sample separation where we can neglect disturbances inside the sample caused by the tip presence.[10,17] We partly avoid this problem by taking the

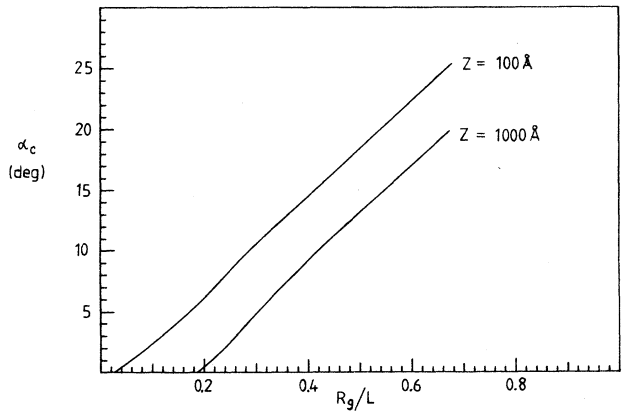

FIG. 6. Relation between R_g/L and critical angle α_c at two z levels. $L = 3000$ Å, R_g varied.

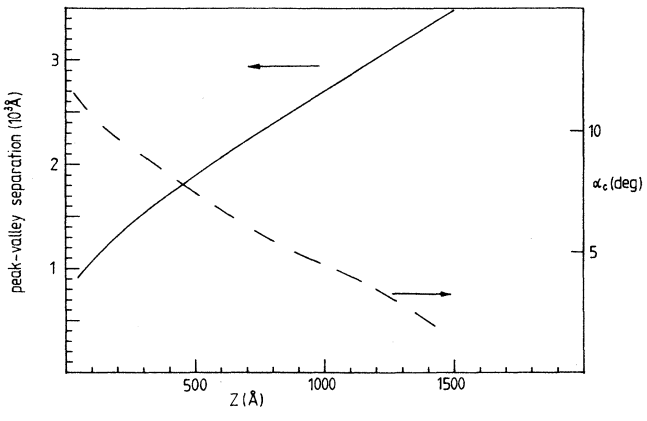

FIG. 8. Dependence of peak-valley separation AB and critical angle α_c vs z height of scanning. $R_g/L = 0.3$, $R_g = 900$ Å, and $L = 3000$ Å.

tip without magnetizing it before the experiment. Then a lateral resolution of better than 100 Å could be achieved.[5,14] In order to explain this result the domain structure of the tip has to be taken into account.[18] The presented theory assumes, however, a uniformly magnetized tip and can be applied successfully to experiments with the use of such a tip. The lateral resolution experimentally observed with the use of such tips is of the order of 1000 Å.[2,4]

From the results of this paper, it is not possible to make a general statement about the best obtainable lateral resolution in MFM. Tips with a domain structure inside make the problem especially difficult to describe. We can obtain the high resolution with such tips but the problem is to control the domain structure inside.[18] Therefore it is obvious that care has to be taken when comparing experimental results obtained with different tips and scanning heights.

III. CONCLUDING REMARKS

All the presented simulations can, of course, be repeated with constant R_g and α. Thus the optimized value of L or R_d can be found. Similarly, R_g and R_d can be kept constant. We then find the highest resolution for $L \rightarrow \infty$, which is not surprising in view of Figs. 6 and 7 and, of course, has the same physical explanation given above for the existence of α_c. In summary, a mathematical approach has been presented to describe MFM as a function of tip geometry (parameters R_g, L, and α) and tip-sample distance z. We find the following results: (1) The magnetic image of a domain pattern with perpendicular anisotropy strongly depends on the direction of the tip magnetization (Fig. 3). (2) Surprisingly, the highest lateral resolution is not related to the tip with the smallest tip radius R_d. (3) At each z level and for each ratio R_g/L there is a critical angle α_c for the highest resolution (Fig. 5). (4) For the same ratio R_g/L but different angles α, the measured sensitivity can differ by more than a factor of 3 (Fig. 5). (5) Critical angles α_c are a nearly linear function of the ratio R_g/L for each z level (Fig. 6). (6) The peak-valley separation AB (lateral resolution) depends nearly linearly on the critical angle α_c for each z level (Fig. 7). (7) The peak-valley separation AB (lateral resolution) strongly depends on the z level (Fig. 8).

We have shown in this paper how geometrically tip parameters influence the highest lateral resolution which can be achieved with the technique of MFM. We have presented theoretical evidence that the lateral resolution and sensitivity strongly depend on geometrical tip parameters. This has to be taken into account when comparing experimental results obtained with different tips. The relevant parameters defining tip geometry and the sample-tip distance are crucial if quantitative information is to be deduced from measured force or compliance curves in MFM experiments.

ACKNOWLEDGMENTS

We would like to thank Professor H.-J. Güntherodt and Professor H. Thomas for fruitful discussions and critical comments. This work was supported by the Swiss National Science Foundation and the Komission zur Förderung der Wissenschaftlichen Forschung.

---

*On leave from the Institute of Physics, Polish Academy of Sciences.

[1]G. Binning, C. F. Quate, and Ch. Gerber, Phys. Rev. Lett. **56**, 930 (1986).

[2]Y. Martin and K. H. Wickramasinghe, Appl. Phys. Lett. **50**, 1455 (1987).

[3]J. J. Saenz, N. Garcia, P. Grütter, E. Meyer, H. Heinzelmann, R. Wiesendanger, L. Rosenthaler, H.-R. Hidber, and H.-J. Güntherodt, J. Appl. Phys. **62**, 4293 (1987).

[4]Y. Martin, D. Rugar, and H. K. Wickramasinghe, Appl. Phys. Lett. **52**, 244 (1988).

[5]P. Grütter, E. Meyer, H. Heinzelmann, L. Rosenthaler, H.-R. Hidber, and H.-J. Güntherodt, J. Vac. Sci. Technol. **A(2)**, 279 (1988).

[6]H. J. Mamin, D. Rugar, J. E. Stern, B. D. Terris, and S. Lambert, Appl. Phys. Lett. **53**, 1563 (1988).

[7]D. Rugar, H. J. Mamin, R. Erlandsson, J. E. Stern, and B. Terris, Rev. Sci. Instrum. **59**, 2337 (1988).

[8]A. Wadas, J. Magn. Magn. Mater. **71**, 147 (1988).

[9]A. Wadas, J. Magn. Magn. Mater. **72**, 293 (1988).

[10]A. Wadas, J. Magn. Magn. Mater. (to be published).

[11]A. Wadas, International Conference on Magnetism, Paris, France, 25–29 July, 1988 (unpublished).

[12]U. Hartmann, J. Microsc. (Oxford) (to be published).

[13]J. J. Saenz, N. Garcia, and J. C. Slonczewski, Appl. Phys. Lett. **53**, 1449 (1988).

[14]P. Grütter, E. Meyer, and H. Heinzelmann, The Twelfth International Colloquim on Magnetic Films and Surfaces, Le Creusot, France, 1–5 August, 1988 (unpublished).

[15]R. Coelho and J. Debeau, J. Phys. D **4**, 1266 (1971).

[16]I. S. Gradshteyn and I. M. Ryzhik, *Tables of Integrals, Series, and Products* (Academic, New York, 1965), p. 197.

[17]U. Hartmann, J. Appl. Phys. **64**, 1561 (1988).

[18]P. Grütter, J. Appl. Phys. (to be published).